The effect of camber control on power consumption during handling manoeuvres

ABSTRACT

Vehicle power consumption is receiving widespread attention in the industry. One of the approaches is to include camber control to reduce power loss during cornering. This approach changes the camber angle during cornering, reducing the steering angle needed. The published literature is limited to semi-empirical tyre models and simplified vehicle models. This investigation uses a physics-based tyre model and a full vehicle model to verify if the power savings reported in the literature are indeed achievable. The simulation results indicate that the reported power savings are indeed possible, but that the power saved during normal driving is limited. It is concluded that camber control is not suited to reducing power consumption during normal driving. A deeper investigation revealed that the use of radial tyres is one explanation for this finding. Camber control is thus not recommended as a power-saving strategy for practical applications using traditional radial tyres.

Keywords: camber angle control, cornering losses, vehicle power saving, handling

1 INTRODUCTION AND BACKGROUND

The burning of fossil fuels is the largest contributor to climate change. Transportation via cars, trucks, ships and planes make up nearly a quarter of global energy-related carbon dioxide emissions (United Nations, n.d.). More efficient vehicles are one of the major steps that can be taken to reduce greenhouse gas emissions. Several aspects contribute to vehicle efficiency, including:

- Improving the utilization of the energy source by the motor. This is done either by improving the efficiency of the internal combustion engine (ICE) (Johnson and Joshi, 2018), or by using hybrid- or battery-powered electric vehicles (EVs) (International Energy Agency, 2021).
- Reducing losses that increase the demand force that needs to be overcome. Contributors to the demand force are drivetrain losses, rolling resistance, aerodynamic drag and vehicle dynamics losses (Jerrelind et al., 2021).

EVs are becoming an increasingly attractive option to consumers, as evidenced by the number of EVs sold. Ten million EVs were on the world's roads in 2020, representing 4.6% of the world-wide vehicle sales (International Energy Agency, 2021). This mass adoption is being driven by global policies targeting CO_2 emissions such as the European Union's Regulation (EU) 2019/631 (European Parliament and the council of the European Union, 2019) and California's Zero-Emission Vehicle Program (California Air Resources Board, 2022). The International Energy Agency predicts that global EV stock will be somewhere between 145 to 225 million units by 2030, with approximately 50% of those vehicles being personal battery-powered EVs and the balance plug-in hybrid EVs (International Energy Agency, 2021).

The percentage of EVs being sold has increased gradually. 700 units were sold in the EU in 2010, but this has risen to about 550 000 units in 2019 (3.5% of new registrations). This number surged in 2020, roughly accounting for 11% of newly registered passenger cars in 2020 (European Environment

Agency, 2021). The gradual market penetration has led to an increasing array of models and options available to the customer (Autocar, 2022). As a result, EVs have increased in size and mass to meet customer demand (European Environment Agency, 2021).

Wang et al. (2020) report that the biggest obstacle to EV adoption is concerns about mileage. Andwari et al. (2017) reviewed the technology readiness level of battery EVs. They list some of the technical challenges faced by battery EVs, including electricity storage, battery charging time, and a lack of charging infrastructure – all of these challenges contribute to the range anxiety experienced by consumers. EV range can be extended by storing more energy, properly managing the stored energy for optimal efficiency, and reducing the parasitic losses associated with energy conversion (from electric to kinetic) and other vehicle dynamics-related losses (such as rolling resistance and aerodynamic drag) (Andwari et al., 2017). Beckers et al. (2020) indicate that the cornering resistance may cause a loss of up to 5.8% for battery electric busses driving in city environments. Reducing tyre slip angle thus represents a viable energy saving method, permitted that acceptable cornering performance can be maintained.

Actively changing the camber angle of some or all of the wheels of a vehicle has not been applied extensively in the vehicle market, although some prototypes exist. Camber is typically controlled by including an actuator in the suspension links to change the suspension geometry (Park and Sohn, 2012, Roethof et al., 2016). This is quite easily done on non-driven wheels, but the presence of driveshafts and CV-joints often limit the application of active camber control on driven wheels – this is a practical challenge faced by traditional, ICE-powered vehicles. However, the use of electric motors presents the opportunity to change the traditional layout of a vehicle. Using in-wheel motors is a popular way of reducing energy losses associated with the mechanical drivetrain – this essentially changes the EV from a traditional centralized powertrain into a distributed actuation system (Chen and Wang, 2013). In-wheel motors also allow for the active change of camber angle on driven wheels. Actively changing camber angle is thus practically feasible and may find wider adoption if the benefits (such as reducing cornering power losses or improved handling) outweigh the cost of increased complexity.

Several studies (Roethof et al., 2016, Braghin et al., 2010, Ammon, 2005, Schiehlen and Schirle, 2006, Jerrelind et al., 2013, Kavitha et al., 2019, Park and Sohn, 2012, Chen and Wang, 2013, Bhat et al., 2017, Davari, 2017, Sun et al., 2017, Sun et al., 2018, Jerrelind et al., 2021) have investigated the effect of changing and controlling the camber angle on steering feel, handling performance and reducing cornering resistance. The interested reader is referred to these publications. Some highlights include:

- Bhat et al. (2017) and Davari (2017) proposed an over-actuation method to improve the cornering efficiency of an EV. The optimal values of slip angle and camber angle were found, and a camber side-slip controller (CSC) was developed. The Extended Brush Tyre Model (EBM) was parameterized and used in combination with either the bicycle model or a three degree-of-freedom (DOF) vehicle model. The energy efficiency during cornering was improved by 13%.
- Sun et al. (2017) investigated the use of camber control and torque vectoring to improve energy efficiency during cornering. They concluded that torque vectoring has a negligible impact on energy reduction, but that an energy saving of up to 14% can be achieved by combining torque vectoring with camber control during steady-state cornering.
- The camber control method proposed by Sun et al. (2018) utilises a relationship between the lateral acceleration and the camber angle as the input to the camber controller. The approach used Magic Formula tyre models for combined slip and camber angles along with a two-track yaw-plane vehicle model. The camber angle of the front wheels and rear wheels were kept

the same (i.e. left and right wheels on each axle are at the same camber angle), but differences between front and rear camber angles were permissible. Based on their analysis, the authors recommended that the same camber angle be used on the front and rear axles. It was concluded that, as the lateral acceleration increased, the potential energy saving increases. The maximum energy saving observed was 22.1%.

Jerrelind et al. (2021) discuss the potential energy savings achievable by including camber control in addition to slip angle control (traditional steering):

- Lateral force generation due to camber angle change is not associated with a significant relaxation length, and hence the lateral force reaches steady-state values almost instantaneously. Handling responsiveness may thus be improved.
- The actuators required for camber control can consume up to 1 kW during a severe double lane change manoeuvre at 99 km/h. The actuators consumed about 1 % of the energy required by the drive motors, thus not an insignificant amount.
- The forces generated by camber control are relatively small and should be seen as additional to the force generated by traditional steering – traditional steering can thus not be replaced by active camber control, rather, active camber control could be used to reduce the steering angle needed.
- Excessive camber angle may lead to higher rolling resistance and increased, uneven tyre wear.

The addition of camber control thus comes at a cost and it warrants further investigation. The existing literature relies on simplified vehicle models (such as a single-track or yaw-plane models) and semi-empirical tyre models (such as the Magic Formula model). The current study makes the following contributions:

- Rather than relying on simplified tyre models, this study uses an experimentally validated physics-based FTire model developed by Wright et al. (2019). The FTire model physically models the contact between the tyre and the road – the contact patch shape changes with a change in camber angle, and hence is much more comprehensive than the single point contact model utilised by typical semi-empirical models (Gipser, 2007).
- An experimentally validated vehicle model containing 16 DOFs is used. The vehicle model was developed in Adams by Thoresson et al. (2009) and includes a hydro-pneumatic suspension model, suspension bushings, body torsion and experimentally determined CG position and mass moments of inertia.

The objective of the current study is to confirm that energy saving is possible by using camber control in addition to traditional steering through using a fully nonlinear vehicle model. If the large savings as reported by Bhat et al. (2017), Davari (2017) and Sun et al. (2018) are achievable, camber control should be seriously considered by vehicle designers as a feasible option to reduce energy losses due to cornering.

2 METHODOLOGY

The methodology followed consists of three steps:

1. Understanding the fundamental causes of power loss during cornering.
2. Investigating the potential energy savings with a single tyre model – this is done with the experimentally validated FTire model running on a simulated drum test rig.

3. The single tyre investigation of step 2 is expanded to a full vehicle model. The full vehicle model is used to develop a simple camber controller and to evaluate the controller's performance.

Table 1 contains the nomenclature used in this study.

Table 1 – Nomenclature

Insert table 1 here

2.1 POWER LOSS DURING CORNERING

During cornering, cornering resistance is experienced because of the side-slip of the tyres and the vehicle. The power due to cornering resistance, P_c, is given by (Jerrelind et al., 2021):

$$P_c = F_c v_x \tag{1}$$

Assuming small slip angles, this can be expanded to each of the four tyres of the vehicle:

$$P_c = F_{y,FL}\alpha_{FL}v_x + F_{y,FR}\alpha_{FR}v_x + F_{y,RL}\alpha_{RL}v_x + F_{y,RR}\alpha_{RR}v_x \tag{2}$$

The lateral tyre forces can be linearized with the cornering stiffness:

$$P_c = C_{\alpha,FL}\alpha_{FL}^2 v_x + C_{\alpha,FR}\alpha_{FR}^2 v_x + C_{\alpha,RL}\alpha_{RL}^2 v_x + C_{\alpha,RR}\alpha_{RR}^2 v_x \tag{3}$$

$$P_c = \left(C_{\alpha,FL}\alpha_{FL}^2 + C_{\alpha,FR}\alpha_{FR}^2 + C_{\alpha,RL}\alpha_{RL}^2 + C_{\alpha,RR}\alpha_{RR}^2\right)v_x \tag{4}$$

$$\therefore F_c = C_{\alpha,FL}\alpha_{FL}^2 + C_{\alpha,FR}\alpha_{FR}^2 + C_{\alpha,RL}\alpha_{RL}^2 + C_{\alpha,RR}\alpha_{RR}^2 \tag{5}$$

Equation (5) shows that the cornering force is proportional to the square of the slip angle.

Equation (1) can also be used as a metric to determine the power loss reduction by any proposed camber control system. Actuation of the camber angle will also require the use of energy. This cannot be neglected when investigating the effect of any active camber control system on the energy efficiency. The power required to control the camber angle is related to overcoming the overturning moment (M_x) of each wheel. Sun et al. (2018) defines this power as:

$$P_{camber} = \begin{cases} \sum_{i=1}^{4} M_{xi}\dot{\gamma}_i, & if \quad M_{xi}\dot{\gamma}_i \geq 0 \\ 0, & if \quad M_{xi}\dot{\gamma}_i < 0 \end{cases} \tag{6}$$

The total power thus consumed during cornering is the summation of the cornering power loss and the cost of controlling the camber angle:

$$P_{loss} = P_c + P_{camber} \tag{7}$$

2.2 SINGLE TYRE INVESTIGATION

2.2.1 Tyre model

As mentioned in the Introduction, one of the specific contributions of this current study is the use of a high fidelity, physics-based tyre model rather than the use of a semi-empirical tyre model as commonly done in the literature. The tyre model used for the study is an FTire model. The FTire model is a three-dimensional and highly nonlinear physics-based model designed to be used in ride comfort and handling simulations. It consists of (1) a flexible ring structural model containing belt elements with stiffness in various directions; (2) a tread model that handles the contact between the tyre and

road, the tyre-road friction, contact patch compliance and ground pressure; and (3) a thermal model (Gipser, 2007). The FTire model goes a step further when determining tyre power loss than just considering the cornering resistance. The power loss due to friction is calculated internally in the model by the dot product of the tyre friction force and the sliding velocity (cosin scientific software, 2022):

$$P_{fric} = \vec{v}_{slide} \cdot \vec{F}_{fric} \tag{8}$$

This definition of the friction power loss thus includes any force acting in the sliding direction and may thus include additional power losses, such as tyre traction losses. Equation (7) is thus updated:

$$P_{loss} = P_{fric} + P_{camber} \tag{9}$$

The tyre used for the study is a Pirelli Scorpion Verde 235/55 R19 105V all-season tyre. Wright et al. (2019) developed and experimentally validated the tyre model's vertical, longitudinal and lateral stiffness on flat plates and over multiple cleats at various camber angles. The model exhibited excellent correlation with experimental measurements for camber angles up to -4°. Figure 1 shows the footprint of the tyre at -4° camber (Wright, 2017).

Insert figure 1 here

Figure 1 – Footprint on a flat surface of Pirelli Scorpion Verde 235/55 R19 105V tyre at -4° camber at 250 kPa inflation pressure (Wright, 2017)

2.2.2 Drum rig simulation

Now that the tyre model has been introduced, the next step is investigating the possible energy savings by adding camber during steering to reduce the cornering resistance. Using a single tyre on a drum rig removes some uncertainty by investigating one aspect at a time. With a full simulation model, other aspects such as load transfer and camber angle change due to body roll will be present.

An Adams (MSC Software, 2016) model of a drum test rig was developed. The drum test rig consists of six rigid bodies and the tyre. It contains five degrees of freedom to allow for various vertical tyre deflections, camber angles and slip angles. The drum can rotate at varying speeds with the tyre rolling freely on the surface of the drum. Figure 2 shows the graphical topology and an isometric view of the drum rig simulation model.

Insert figure 2 here

Figure 2 – Graphical topology of drum rig simulation model (left) and isometric view of model in Adams (right)

Simulations were performed at a constant rotational speed at various vertical loads and combinations of tyre slip and camber angles. The model provided the lateral force generated and friction power loss (Equation (8)) as output. Table 2 lists the simulation inputs used. During the simulations, the camber angle was kept constant, hence the power required to change the camber angle was not included in this section of the investigation (refer to Equation (6)). The rate of camber angle change is zero and hence the power consumed is zero.

Table 2 – Drum rig simulation inputs

Insert table 2 here

Figure 3(a) shows the lateral tyre force for the range of inputs in Table 2 at a vertical load of 3500 N. It is evident that the inclusion of camber increases the lateral force, as expected. Figure 3(b) shows the friction power loss determined by the tyre model. Lines of constant slip angle are indicated with black dashed lines. The results in Figure 3(b) indicate that a significant amount of power can be saved

by reducing the slip angle and including some camber angle. Two data points are highlighted in Figure 3(b) to illustrate this. To generate a lateral force of approximately 3000 N, a pure slip angle (with no camber angle) of 7° is needed. By adding 6° of camber angle, the slip angle can be reduced to 5°. The result is a reduction in friction power loss from 3 kW to 2 kW. This represents a saving of 33%. At very high lateral forces approaching the friction limit at 3500 N (recall that the vertical load is 3500 N), the potential energy saving by adding camber is significant. This is, however, the extreme case. It is not expected that the typical driver will approach a lateral acceleration of 1g, at least not for any significant amount of time.

Insert Figure 3 here

Figure 3 – (a) Lateral force versus slip angle for three camber angles at a vertical load of 3500 N (b) Friction power loss as a function of lateral force at various camber angles at a vertical load of 3500 N

Figure 4 shows the potential power savings in terms of percentage friction power reduced for all the simulations run with the drum model according to the inputs listed in Table 2. The percentage power saved is defined as the percentage of power saved by adding camber angle compared to the baseline case where the camber angle is zero. Several observations are made:

- The results in Figure 3 and Figure 4 indicate that the power reduction is significant at high lateral forces.
- At low lateral forces, the inclusion of camber angle results in an increase in friction power loss. This is because of the tyre scrubbing and asymmetric deformation of the contact patch. The cornering resistance at low lateral forces (and thus small slip angles) is very small, hence adding camber control at small slip angles increases power consumption instead of reducing it.
- The benefit of adding camber angle to slip angle is increased at lower vertical loads. This may have implications when lateral load transfer is present during real driving scenarios. This indicates that lateral load transfer should be considered when evaluating the potential energy savings of active camber control.

Insert figure 4 here

Figure 4 – Power reduction possible by adding camber angle to slip angle at various tyre lateral forces and vertical tyre loads (image cropped to indicate power savings)

The drum rig simulation results indicate that a significant amount of power can be saved by including camber angle in addition to tyre slip angle at high lateral forces or slip angles. This confirms the results found in the literature and discussed earlier. The use of a high fidelity FTire model in this initial part of the investigation gives further confidence that power savings may be realized. The power savings indicated here may be an over exaggeration, because the tyre is simulated in a highly controlled environment where no load transfer or body roll is present and the power needed to change the camber angle is neglected. The combined effect when using a full vehicle model will be investigated using real driving scenarios. It is expected that the power savings on the full vehicle analysis will not be as significant as found during the drum rig simulations.

2.3 FULL VEHICLE MODEL INVESTIGATION

A nonlinear full vehicle model, developed and extensively validated by Thoresson et al. (2009) was used as the vehicle model for the full vehicle simulation studies. The vehicle model was developed in Adams and is based on a Land Rover Defender 110 Tdi. The vehicle model includes a non-linear driver model that is used for path following and braking (Kapania and Gerdes, 2015, Hamersma and Els,

2014). The test vehicle is equipped with a semi-active hydro-pneumatic suspension system that can change the spring and damper characteristics at each corner of the vehicle. The suspension can be used in 'Handling' mode (all four springs stiff with high damping) or in 'Ride Comfort' mode (all four springs soft with low damping) (Theron and Els, 2007). The full vehicle model was validated against experimental results by a previous study (Peenze, 2019) using a Magic Formula tyre model.

Two changes to the full vehicle model were necessary before further investigation was possible:

1. The Magic Formula tyre model used by Peenze (2019) was replaced with the FTire model of the Pirelli Scorpion Verde 235/55 R19 105V that was used in the drum rig simulation model. The biggest difference between the two tyres is the aspect ratio. The original tyre has an aspect ratio of 85% and is relatively insensitive to camber changes because of the tyre carcass compliance. The Magic Formula tyre model of the original tyre was not parameterised for camber angle changes. The Pirelli tyre used in this study has a much lower aspect ratio (55%) and its carcass is much stiffer than the original tyre. The Pirelli tyre was chosen for this study because of its increased sensitivity to camber angle changes.
2. Camber degrees of freedom had to be included at each wheel to allow for actuation of the camber angle.

A cross validation was conducted with the original vehicle model and with experimental data gathered by Peenze (2019) to ensure the modified vehicle model still gives acceptable results. Three models were used for the cross validation:

1. The **baseline** model – the full vehicle without any modifications as used by (Peenze, 2019), including the original Magic Formula tyre model.
2. The **modified baseline** model – this model replaces the original Magic Formula tyre model with the FTire model of the Pirelli tyre.
3. The **camber** model – this model includes the camber degrees of freedom at each wheel and the FTire model.

The cross validation was conducted by taking the exact same simulation inputs that was used by Peenze (2019) and comparing the model response when performing a severe double lane change manoeuvre (as defined by ISO3888:-1:1999 (International Organisation of Standardisation, 1999)) at 70km/h with the suspension in the 'Handling' mode. Figure 5 compares the three models' response with experimental data from Peenze (2019). Excellent correlation between the various measurements and experimental data can be seen, even with the introduction of a new tyre model. It was not anticipated that the introduction of the camber degree of freedom would have any effect on the simulation results, as the camber angle was kept at 0° during the validation simulations. It is clear in Figure 5 that the solid green line (modified baseline model) and the dashed black line (camber model) are coincident as expected. The negligible impact of changing the tyre model from the original Magic Formula to the FTire model of the Pirelli tyre is surprising. The validation results instil confidence in the simulation results obtained with the full vehicle model used from this point forward.

Insert figure 5 here

Figure 5 – Comparison of severe double lane change simulation results for baseline, modified baseline and camber models with experimental data gathered on test vehicle in baseline configuration.

Now that the full vehicle model has been validated, it can be used to investigate the effect of load transfer, the resulting roll angle and the inclusion of wheel drive torque on the potential power savings that adding camber angle to the slip angle could achieve. All four wheels of the vehicle are driven with torques applied to the wheel hubs. The test vehicle the vehicle model is based on has open

differentials at both axles and hence the drive torque is evenly distributed to all four wheels. From this point forward, only the camber model will be used.

A series of constant radius (CR) simulations were conducted at gradually increasing vehicle speeds at passive camber angles. All wheels were set to the same camber angle, with the wheels leaning into the turn (as a motorcycle driver would do when negotiating a corner). A radius of 50 m was used and the vehicle speed gradually increased from 0 to 72 km/h (20 m/s) over a period of 100s. The camber angle for all four wheels were kept the same and simulations were run at 0.5° increments from 0° to 5° camber and then 6°, 7° and 8°. The camber angle is relative to the axle, and does not represent the angle with the road. The test vehicle does not induce king pin angle change with steer angle change – the steering kinematics simply do not allow for that, because the test vehicle has solid axles in both the front and rear of the vehicle. Camber control is achieved by controlling the relative angle between the wheel and the axle – this may also be called king pin inclination angle control. By default, the test vehicle king pin inclination angle is zero. The test vehicle's wheels are thus perpendicular to the road surface when stationary.

Absolute camber angle will change as load is transferred from the inside wheels to the outside wheels, resulting in higher tyre deflection on the outside and lower tyre deflection on the inside – effectively rolling the axles. The simulation results indicate that the change in absolute camber angle due to this effect is approximately 1° for the front axle and 0.75° for the rear axle (from 0 g lateral acceleration to 0.77 g).

For the constant radius test results, such as those in Figure 6, -4° camber angle indicates that the angle between the wheel and the axle was set to -4° for the duration of the simulation. The results in Figure 7, where camber angle is shown on the x-axis, are for this relative angle between wheel and axle. It must be noted that the friction power calculation is obtained from the FTire model, which naturally uses the absolute camber angle in the simulation and thus includes the effect of axle roll in the results.

Figure 6 shows an example of the constant radius test results – this specific run was conducted at -4° camber angle. As expected, the lateral acceleration and body roll angle gradually increase as the speed increases. Because the speed increase is gradual, the constant radius test is seen as a quasi-static manoeuvre. Similarly, the total friction power loss (summed for all four tyres) increases as the lateral acceleration increases. This indicates that the contact patch starts sliding; significant power is lost due to the sliding of the contact patch, up to 40 kW at very high lateral accelerations (7.5 m/s^2).

Insert figure 6 here

Figure 6 - Constant radius test simulation results at -4° camber

The constant radius test results were processed to determine the possible energy savings that could be achieved by adding camber angle to steering. Two metrics are used, firstly the difference in friction power compared to the baseline case (zero camber taken as baseline case), and secondly the percentage power reduction compared to the baseline case. The simulation data were processed according to the following steps:

1. Some outliers were seen in the initial few simulation time steps. These outliers were manually removed from the dataset. The outliers are present because the simulation model does not start from a static equilibrium condition.
2. Once outliers have been removed, a spline is fit to the friction power loss vs. lateral acceleration graph using MATLAB's Curve Fit Toolbox (MathWorks, 2016).
3. Steps 1 and 2 are repeated for all constant radius curve simulations.

4. At this point, a comparison between the baseline case and the simulation runs with camber angle can begin using the fitted curves.

Figure 7(a) shows the change in power possible by adding camber angle and Figure 7(b) shows the percentage power saved.

Insert figure 7 here

Figure 7 - (a) Change in power loss during constant radius tests; (b) percentage power saved during constant radius tests

The results in Figure 7 give insight that the single tyre investigation could not provide on its own. Several key findings are made based on these results:

- By combining camber angle and steering input, a reduction in power lost due to friction can be achieved. This confirms the findings in the literature discussed in Section 1.
- There is an optimal amount of camber angle to add and this influenced by the lateral acceleration of the vehicle. Too much camber angle will increase losses, rather than reducing losses.
- The total reduction in power is not significant. Although the percentage power saved can be as much as 11% as shown in Figure 7(b), this is at very low lateral accelerations.
    - This may be beneficial in low speed scenarios such as parking lot manoeuvres, but closer inspection of the actual power saving at these low lateral accelerations in Figure 7(a) indicates that the power saved is less than 50 W. Figure 7(a) indicates a maximum saving of 460 W is possible with the addition of a 3° camber angle at 5.6 m/s^2 lateral acceleration.
    - Hugemann and Nickel (2003) investigated typical accelerations measured during driving. The majority of drivers stay below 3 m/s^2. Figure 7(a) indicates that the total power saved at 3 m/s^2 is a mere 130 W. This excludes the power needed to actively change the camber angle. The use of actuators to change camber angle thus seems infeasible, as the actuators will likely consume more energy than can be saved by adding camber angle. The traditional approach of using a multi-link suspension system that changes the camber angle as the steering input changes is the only feasible approach to realise power savings.
    - Significant power savings are thus limited to highly dynamic manoeuvres, such as a severe double lane change. The potential of saving power to address the range anxiety experienced by EV owners by changing the camber angle is thus limited.

To confirm these conclusions, the results in Figure 7(a) were used to design a camber controller. This has been done in the literature (Sun et al., 2018), where a camber angle setpoint was determined as a function of lateral acceleration. Figure 8 shows the maximum power savings as a function of lateral acceleration and the derived camber angle controller describing the camber angle setpoint as a function of lateral acceleration. It must be noted that this approach still relies on an actuator that changes the camber angle according to the measured lateral acceleration.

Insert figure 8 here

Figure 8 – Maximum power savings derived from Figure 7(a) and proposed camber angle setpoint

The camber angle controller shown in Figure 8 was implemented in the full vehicle model. A running average of the lateral acceleration over a period of 200 ms was used as input and the corresponding camber angle was then prescribed according to the relationship shown in Figure 8. No actuator dynamics were included. Two severe double lane change simulations were run, one at 50 km/h and

the other at 80 km/h. The 50 km/h manoeuvre had a peak lateral acceleration of 2.9 m/s^2 and the 80 km/h manoeuvre peaked at 7.5 m/s^2. The slower manoeuvre thus represents typical city driving acceleration limits and the high-speed manoeuvre represents the limit handling scenario. Figure 9 shows the potential power savings for these manoeuvres.

The results in Figure 9 confirm the observations made earlier that adding active camber control is an ineffective method to reduce the energy consumption of a vehicle. For the 50 km/h scenario, the power savings are less than 600 W for fleeting instances during the double lane change manoeuvre. Even for the high-speed manoeuvre, where lateral accelerations close to the limit of lateral stability are measured and the contact patch is at the point of saturation, the power savings are limited to around 4 kW, representing a peak power saving of approximately 13%. Because actuator dynamics were not included in these simulations, the power consumption of adding an actuator to actively change the camber angle still needs to be accounted for. This emphasizes the impracticality of adding active camber control to improve the energy efficiency of a vehicle.

Insert figure 9 here

Figure 9 – Comparison of friction power loss and potential savings during severe double lane change manoeuvres at 50 km/h ((a) and (c)) and 80 km/h ((b) and (d))

3 DISCUSSION

This study set out to investigate whether the power savings obtainable by adding camber angle control to traditional steering were indeed obtainable when using a physics-based tyre model and when a full vehicle model was used. Initial results using only a single tyre on a drum test rig confirmed that significant power savings were indeed possible. The full vehicle simulation results, however, indicated that the power savings were limited when considering typical driving limits (i.e. lateral acceleration below 3 m/s^2).

The limited power savings of the full vehicle simulations warranted a deeper investigation into the disappointing results. Several poignant observations providing insight were revealed during this deeper investigation:

- The power savings indicated by the single tyre study (c.f. Figure 3b) only become significant at relatively high lateral forces. The difference between the 0° camber and 6° camber simulations becomes apparent when the lateral force generated exceeds 2500 N at a vertical load of 3500 N. This represents a lateral acceleration of 7 m/s^2, much higher than a typical driver will regularly experience during daily driving. The steering angle of the full vehicle model during the severe double lane change manoeuvre at 50 km/h did not exceed 3°. The limited effect of adding camber during 3° steering angle is clear in Figure 3b.
- Reporting only the percentage of power saved is an incomplete metric. The percentage of power saved should be accompanied by the baseline case power consumption or with the actual power saved. Including the actual amount of power saved clearly showed that the inclusion of an actuator to control camber angle will negate any potential energy savings.

A fundamental question that has remained unanswered up to this point is ‘Why does the inclusion of a camber angle have such a small effect on the cornering efficiency?’. The effect of adding camber is, after-all, fundamental to the cornering ability of single-track vehicles such as motorcycles. It was thus expected that adding camber would make a larger contribution to the cornering efficiency. There are

several reasons why adding camber angle to car tyres has an almost negligible effect on cornering efficiency, but the opposite is true for motorcycle tyres:

- Milliken (2006) reports that their tests indicated that the small contact patch of motorcycle tyres results in limited lateral force generation due to slip angle, camber plays the primary role during cornering. Because the CG of a single-track vehicle moves when the driver leans during cornering, the resultant force on the tyres must pass through the CG to achieve equilibrium. Leaning when cornering is thus necessary to not only corner with a motorcycle, but also to achieve equilibrium.
- In his seminal work on the fundamentals of vehicle dynamics, Gillespie (1992) uses the concepts of cornering coefficient and camber coefficient. The cornering coefficient is the cornering stiffness normalized by the vertical load. Similarly, the camber coefficient is the camber stiffness normalized by the vertical load. Gillespie (1992) reports that the typical range of cornering coefficient for radial tyres is in the range of 0.11 to 0.19 N/N/°. This means that for every 1 N of vertical load, for 1° of slip angle, a typical radial tyre will generate approximately 0.15 N of lateral force. In contrast, the camber coefficient for a radial tyre typically lies between 0.002 and 0.018 N/N/°. Thus, for every 1 N of vertical load, for 1° of camber angle, a typical radial tyre will generate 0.01 N of lateral load. The implication is that a typical radial tyre is an order of magnitude more sensitive to steer input than to applied camber angle, especially during manoeuvres requiring 'normal' lateral acceleration.

4 CONCLUSION AND RECOMMENDATIONS

The inclusion of active camber control to improve various aspects of driving have been widely investigated and reported on, but very few studies have made use of physics-based, experimentally validated tyre models along with fully nonlinear three-dimensional vehicle models. Several studies report significant reductions in friction loss during cornering by adding active camber control. This study investigated whether these savings were attainable when using an experimentally validated FTire model together with an experimentally validated vehicle model. Although similar percentage power savings were found, the actual power saved during normal driving manoeuvres was limited to 600 W in total. It is anticipated that the power consumption needed to control the camber angle with an actuator will exceed this and thus limit the value such added complexity would bring to reduce cornering power loss.

A deeper investigation into the fundamentals of tyre cornering and camber sensitivity indicated that radial tyres, as typically used on road going vehicles, are an order of magnitude less sensitive to changes in camber angle than to changes in steer angle. This implies that very large camber angles will be needed to realise any significant power savings. The addition of active camber control is thus not recommended from an energy saving point-of-view.

This study has some limitations, some of which my warrant further investigation:

- The full vehicle model was driven by all four wheels. It is possible that the power saved when cambering non-driven wheels may be more significant.
- The use of active camber angle control to achieve other goals such as improved handling and reduced tyre wear cannot be excluded based on this study's results. It may be worthwhile to investigate the potential improvements achievable by maintaining an absolute zero camber angle during all driving scenarios (i.e. the tyre remains perfectly upright all the time).

- The continued emphasis on reducing rolling resistance to improve EV range has resulted in new tyre designs, typically large diameter, low profile, very narrow tyres. This almost resembles a motorcycle tyre and may have a different camber coefficient. The narrow tyre may also limit the lateral force generation possible, thus necessitating the use of camber thrust to provide additional lateral force during emergency/evasive manoeuvres.
- The benefits reported in this study may be achieved by the development of a multi-link suspension that includes a mechanism to change camber angle along with steering angle. This would remove the need for the inclusion of a power consuming actuator that actively changes the camber angle. However, the possible increased consumption of the power steering system should be considered in such a case.

5 REFERENCES

AMMON, D. 2005. Vehicle dynamics analysis tasks and related tyre simulation challenges. *Vehicle System Dynamics,* 43**,** 30-47.

ANDWARI, A. M., PESIRIDIS, A., RAJOO, S., MARTINEZ-BOTAS, R. & ESFAHANIAN, V. 2017. A review of Battery Electric Vehicle technology and readiness levels. *Renewable and Sustainable Energy Reviews,* 78**,** 414-430.

AUTOCAR. 2022. *New electric cars 2022: what's coming when* [Online]. Available: https://www.autocar.co.uk/car-news/new-cars/new-electric-cars-2022-whats-coming-when [Accessed 10 May 2022].

BECKERS, C. J., BESSELINK, I. J. & NIJMEIJER, H. 2020. Assessing the impact of cornering losses on the energy consumption of electric city buses. *Transportation Research Part D: Transport and Environment,* 86**,** 102360.

BHAT, S., DAVARI, M. M. & NYBACKA, M. 2017. Study on energy loss due to cornering resistance in over-actuated vehicles using optimal control. *SAE International Journal of Vehicle Dynamics, Stability, and NVH,* 1.

BRAGHIN, F., PRADA, A. & SABBIONI, E. Potentialities of active suspensions for the improvement of handling performances. Engineering Systems Design and Analysis, 2010. 235-242.

CALIFORNIA AIR RESOURCES BOARD. 2022. *Zero-emission vehicle program* [Online]. Available: https://ww2.arb.ca.gov/our-work/programs/zero-emission-vehicle-program/about [Accessed 10 May 2022].

CHEN, Y. & WANG, J. 2013. Design and experimental evaluations on energy efficient control allocation methods for overactuated electric vehicles: Longitudinal motion case. *IEEE/ASME Transactions on Mechatronics,* 19**,** 538-548.

COSIN SCIENTIFIC SOFTWARE. 2022. *FTire - Flexible Structure Tire Model Modelization and Parameter Specification* [Online]. Available: https://www.cosin.eu/support/documentation/ [Accessed 11 May 2022].

DAVARI, M. M. 2017. *Exploiting over-actuation to reduce tyre energy losses in vehicle manoeuvres.* KTH Royal Institute of Technology.

EUROPEAN ENVIRONMENT AGENCY. 2021. *New registrations of electric vehicles in Europe* [Online]. Available: https://www.eea.europa.eu/ims/new-registrations-of-electric-vehicles [Accessed 10 May 2022].

EUROPEAN PARLIAMENT AND THE COUNCIL OF THE EUROPEAN UNION. 2019. *Regulation (EU) 2019/631 of the European Parliament and of the council of 17 April 2019 setting CO2 emission perfromance standards for new passenger cars and for new light commercial vehicles, and repealing Regulations (EC) No 443/2009 and (EU) No 510/2011* [Online]. Available: https://eur-lex.europa.eu/eli/reg/2019/631/oj/eng [Accessed 10 May 2022].

GILLESPIE, T. D. 1992. *Fundamentals of vehicle dynamics,* Warrendale, PA, SAE International.

GIPSER, M. 2007. FTire – the tire simulation model for all applications related to vehicle dynamics. *Vehicle System Dynamics,* 45**,** 139-151.

HAMERSMA, H. A. & ELS, P. S. 2014. Longitudinal vehicle dynamics control for improved vehicle safety. *Journal of Terramechanics,* 54**,** 19-36.

HUGEMANN, W. & NICKEL, M. Longitudinal and lateral accelerations in normal day driving. 6th International Conference of The Institute of Traffic Accident Investigators, 2003.

INTERNATIONAL ENERGY AGENCY. 2021. *Global EV Outlook 2021* [Online]. Paris. Available: https://www.iea.org/reports/global-ev-outlook-2021 [Accessed 10 May 2022].
INTERNATIONAL ORGANISATION OF STANDARDISATION 1999. ISO 3888-1:1999 Passenger Cars -- Test track for a severe lane-change manoeuvre -- Part 1: Double lane-change. Geneva, Switzerland.
JERRELIND, J., ALLEN, P., GRUBER, P., BERG, M. & DRUGGE, L. 2021. Contributions of vehicle dynamics to the energy efficient operation of road and rail vehicles. *Vehicle System Dynamics,* 59**,** 1114-1147.
JERRELIND, J., EDRÉN, J., LI, S., DAVARI, M. M., DRUGGE, L. & STENSSON TRIGELL, A. Exploring active camber to enhance vehicle performance and safety. 23rd International Symposium on Dynamics of Vehicles on Roads and Tracks, 19th-23rd of August 2013, Qingdao, China, 2013.
JOHNSON, T. & JOSHI, A. 2018. Review of Vehicle Engine Efficiency and Emissions. *SAE International Journal of Engines,* 11**,** 1307-1330.
KAPANIA, N. R. & GERDES, J. C. 2015. Design of a feedback-feedforward steering controller for accurate path tracking and stability at the limits of handling. *Vehicle System Dynamics,* 53**,** 1687-1704.
KAVITHA, C., SHANKAR, S. A., KARTHIKA, K., ASHOK, B. & ASHOK, S. D. 2019. Active camber and toe control strategy for the double wishbone suspension system. *Journal of King Saud University-Engineering Sciences,* 31**,** 375-384.
MATHWORKS. 2016. *MATLAB and Simulink* [Online]. Available: http://www.mathworks.com/ [Accessed 20 July 2016].
MILLIKEN, W. F. 2006. *Equations of Motion: adventure, risk and innovation: then engineering autobiography of William F Milliken,* Cambridge, MA, USA, Bentley Publishers.
MSC SOFTWARE. 2016. *Adams* [Online]. MSC Software Corporation. Available: http://www.mscsoftware.com/product/adams [Accessed 18 July 2016].
PARK, S.-J. & SOHN, J.-H. 2012. Effects of camber angle control of front suspension on vehicle dynamic behaviors. *Journal of Mechanical Science and Technology,* 26**,** 307-313.
PEENZE, A. J. 2019. *Model predictive suspension control on off-road vechicles.* Dissertation (MEng), University of Pretoria.
ROETHOF, D., SEZER, T., ARAT, M. A. & SHYROKAU, B. 2016. Influence of active camber control on steering feel. *SAE International Journal of Passenger Cars-Mechanical Systems,* 9**,** 124-134.
SCHIEHLEN, W. & SCHIRLE, T. 2006. Modeling and simulation of hydraulic components for passenger cars. *Vehicle System Dynamics,* 44**,** 581-589.
SUN, P., STENSSON TRIGELL, A., DRUGGE, L., JERRELIND, J. & JONASSON, M. 2018. Exploring the potential of camber control to improve vehicles' energy efficiency during cornering. *Energies,* 11**,** 724.
SUN, P., TRIGELL, A. S., DRUGGE, L., JERRELIND, J. & JONASSON, M. 2017. Analysis of camber control and torque vectoring to improve vehicle energy efficiency. *The Dynamics of Vehicles on Roads and Tracks.* CRC Press.
THERON, N. J. & ELS, P. S. 2007. Modelling of a semi-active hydropneumatic spring-damper unit. *International Journal of Vehicle Design,* 45**,** 501-521.
THORESSON, M. J., UYS, P. E., ELS, P. S. & SNYMAN, J. A. 2009. Efficient optimisation of a vehicle suspension system, using a gradient-based approximation method, Part 1: Mathematical modelling. *Mathematical and Computer Modelling,* 50**,** 1421-1436.
UNITED NATIONS. n.d. *Causes and Effects of Climate Change* [Online]. Available: https://www.un.org/en/climatechange/science/causes-effects-climate-change [Accessed 28 Sept 2022].
WANG, Z., CHING, T. W., HUANG, S., WANG, H. & XU, T. 2020. Challenges faced by electric vehicle motors and their solutions. *IEEE Access,* 9**,** 5228-5249.
WRIGHT, K. R. S. 2017. *The Effects of Age and Wear on the Stiffness Properties of an SUV tyre.* Dissertation (MEng), University of Pretoria.
WRIGHT, K. R. S., BOTHA, T. R. & ELS, P. S. 2019. Effects of age and wear on the stiffness and friction properties of an SUV tyre. *Journal of Terramechanics,* 84**,** 21-30.

Table 1 – Nomenclature

Symbol	Description	Unit
$C_{\alpha,i}$	Cornering stiffness at each wheel	N/°
F_c	Cornering force	N
F_y	Lateral force	N
F_{fric}	Resultant friction force in the contact patch	N

M_{xi}	Overturning moment at each wheel of the vehicle	Nm
P_c	Cornering power loss	W
P_{camber}	Camber actuation power consumption	W
P_{fric}	Friction power loss	W
P_{loss}	Total power loss due to cornering and camber actuation	W
v_{slide}	Contact patch sliding velocity	m/s
v_x	Vehicle longitudinal speed	m/s
α_i	Tyre slip angle at each wheel of the vehicle	°
$\dot{\gamma}_i$	Rate of camber angle change at each wheel of the vehicle	°/s

Table 2 – Drum rig simulation inputs

Test Parameter	**Value**	**Units**
Drum Rotational Speed	10	[rad/s]
Drum Diameter	1.6	[m]
Drum Road Longitudinal Speed	3.71	[m/s]
Camber Angle (γ)	0, -1, -2, -3, -4, -5, -6, -7, -8	[°]
Slip Angle (α)	0, 1, 2, 3, 4, 5, 6, 7, 8, 9, 10, 11, 12, 13, 14, 15	[°]
Vertical Applied Load (F_z)	3500 & 6850	[N]

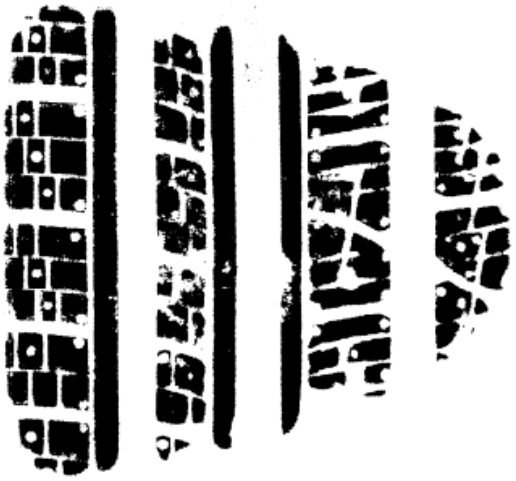

Figure 1 – Footprint on a flat surface of Pirelli Scorpion Verde 235/55 R19 105V tyre at -4° camber at 250kPa inflation pressure (Wright, 2017)

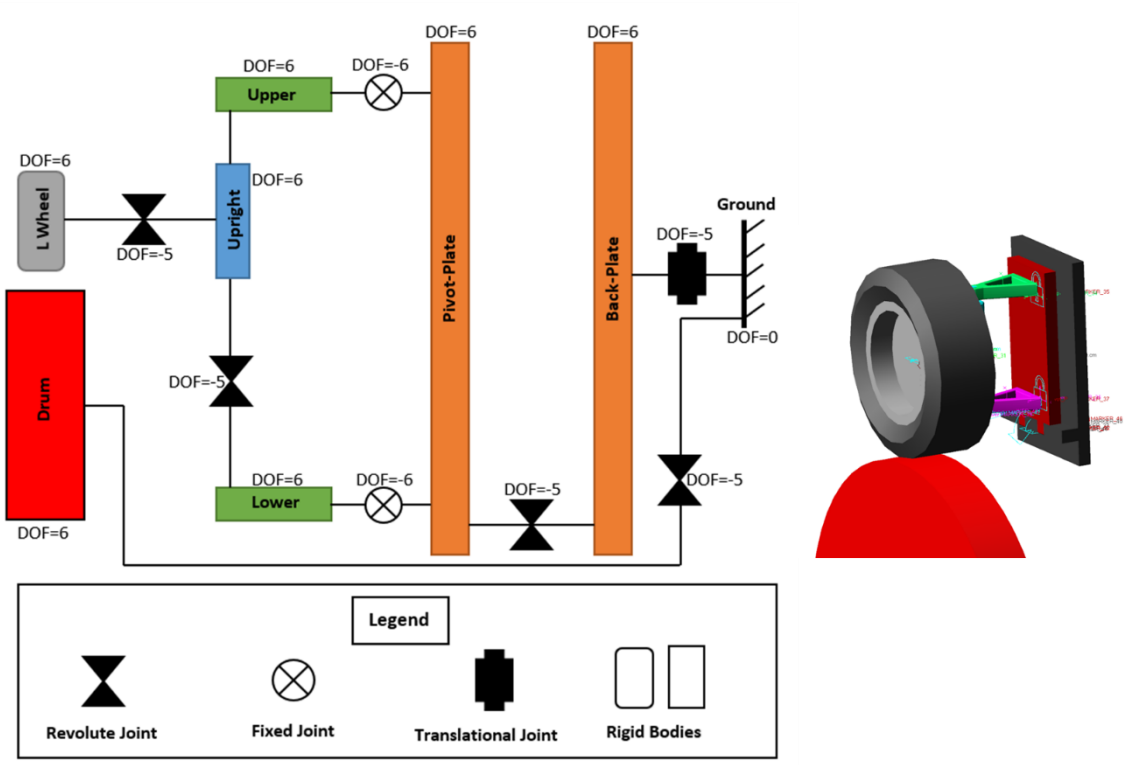

Figure 2 – Graphical topology of drum rig simulation model (left) and isometric view of model in Adams (right)

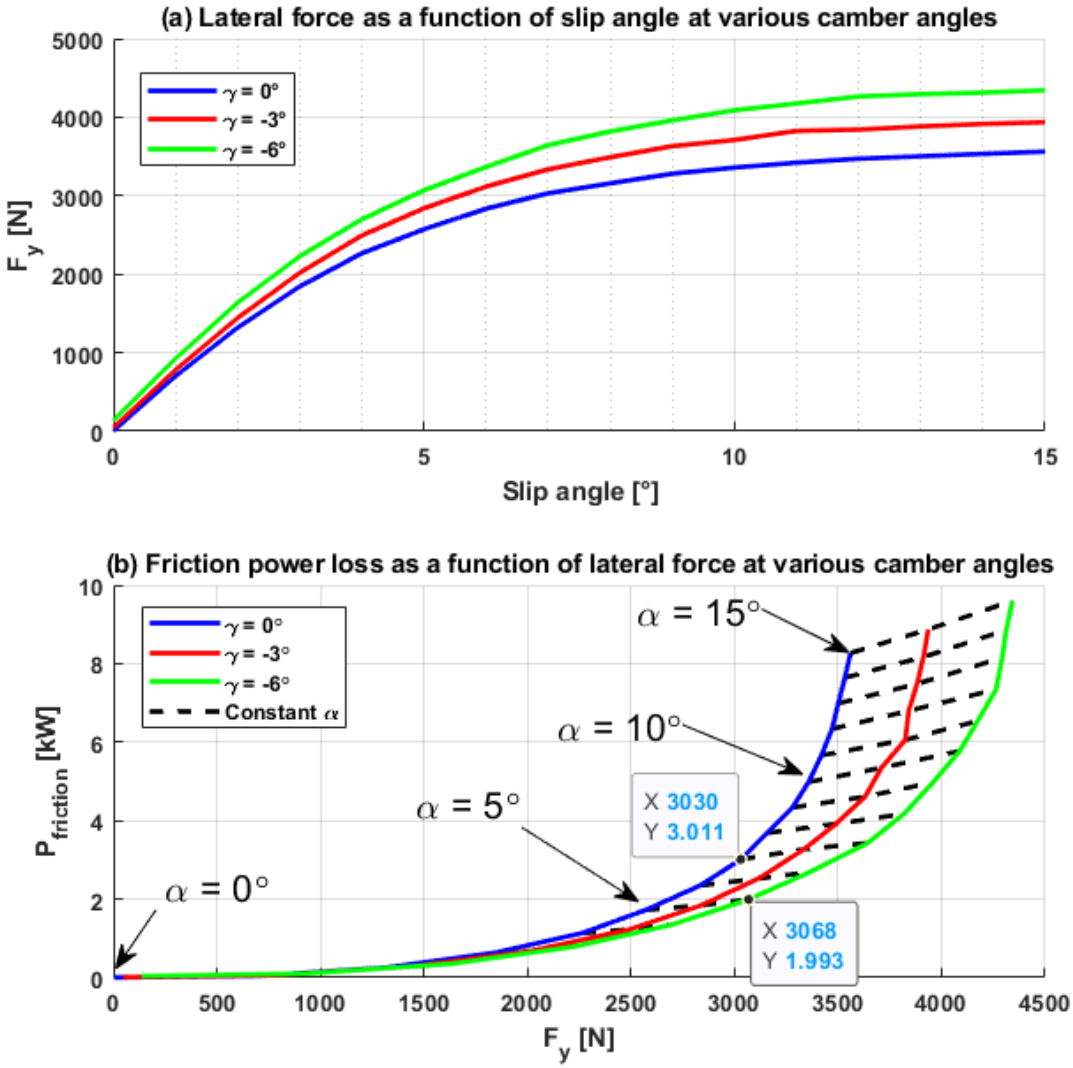

Figure 3 – (a) Lateral force versus slip angle for three camber angles at a vertical load of 3500 N (b) Friction power loss as a function of lateral force at various camber angles at a vertical load of 3500 N

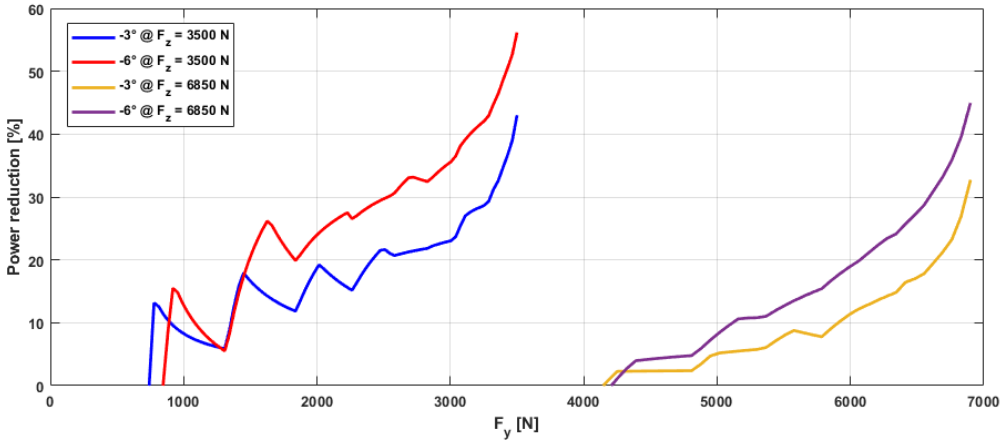

Figure 4 – Power reduction possible by adding camber angle to slip angle at various tyre lateral forces and vertical tyre loads (image cropped to indicate power savings)

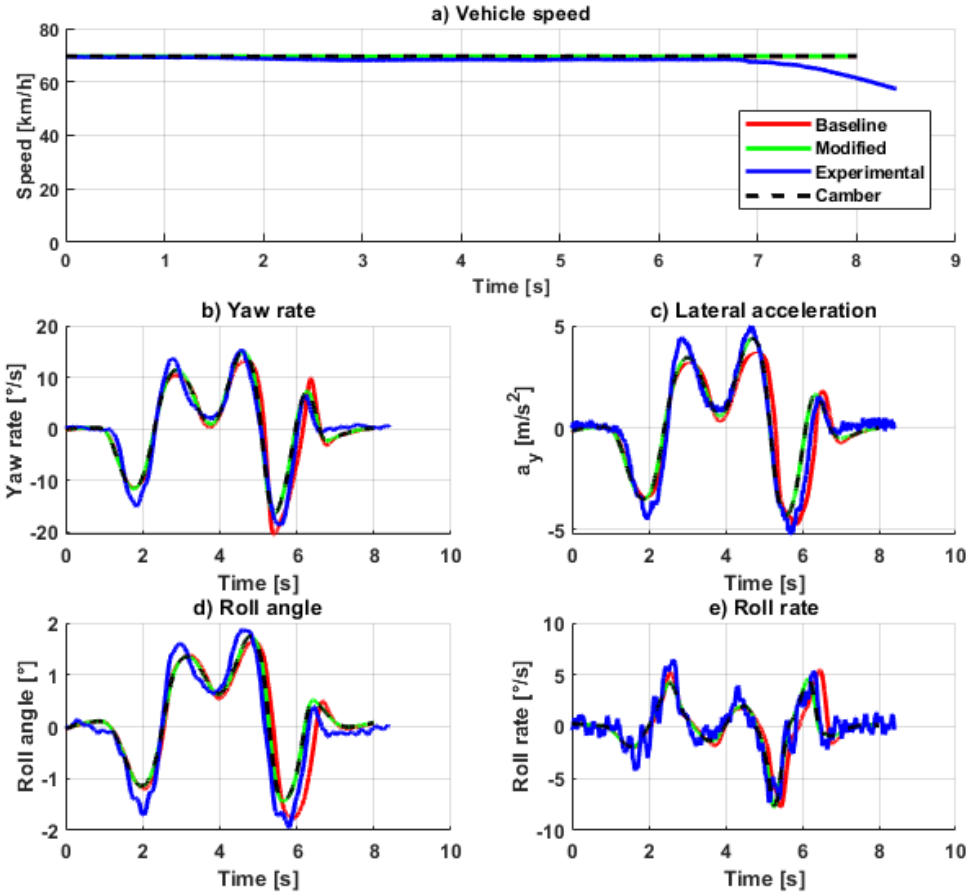

Figure 5 – Comparison of severe double lane change simulation results for baseline, modified baseline and camber models with experimental data gathered on test vehicle in baseline configuration.

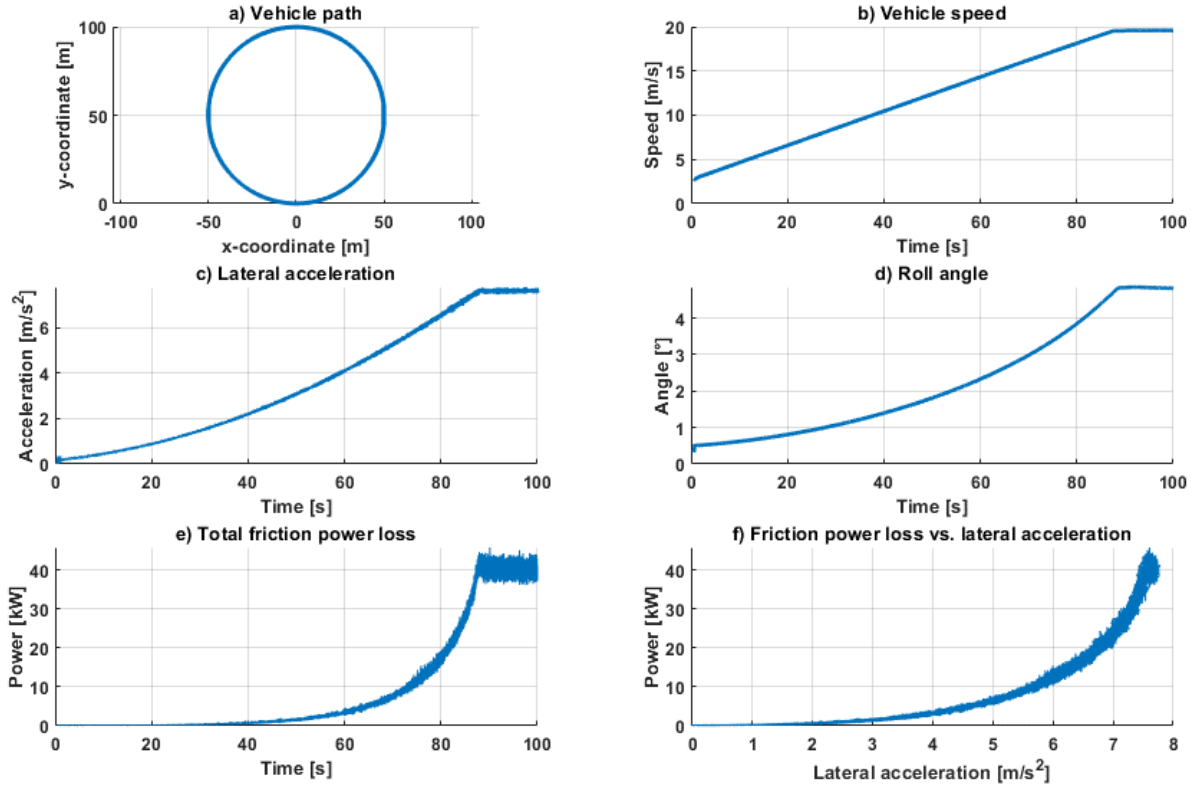

Figure 6 - Constant radius test simulation results at 4° camber

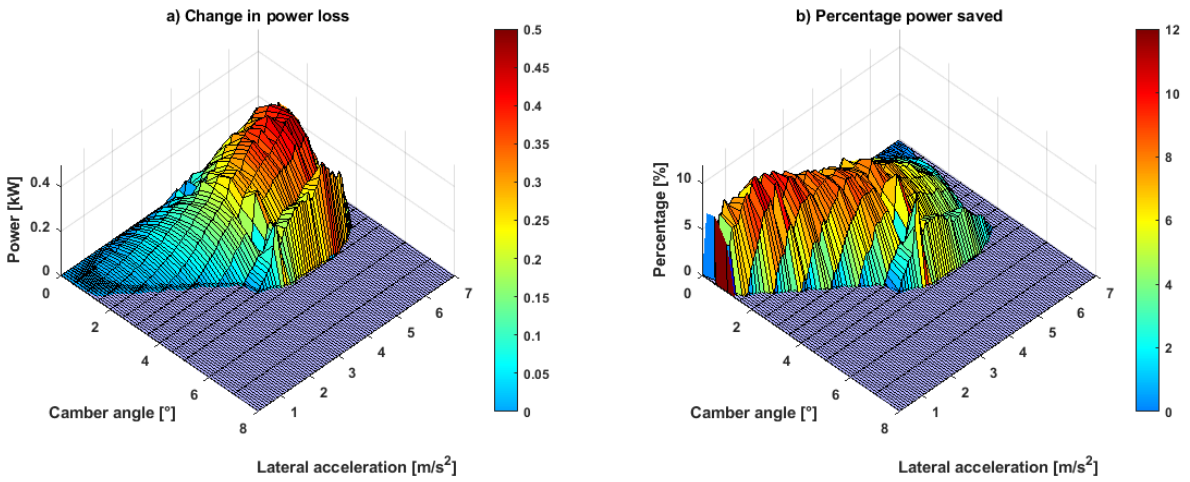

Figure 7 - (a) Change in power loss during constant radius tests; (b) percentage power saved during constant radius tests

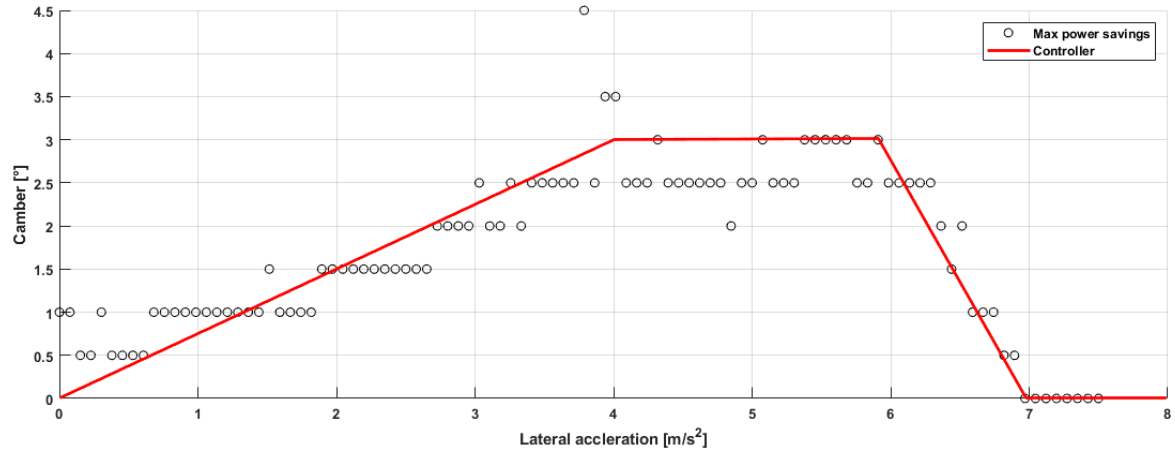

Figure 8 – Maximum power savings derived from Figure 7(a) and proposed camber angle setpoint

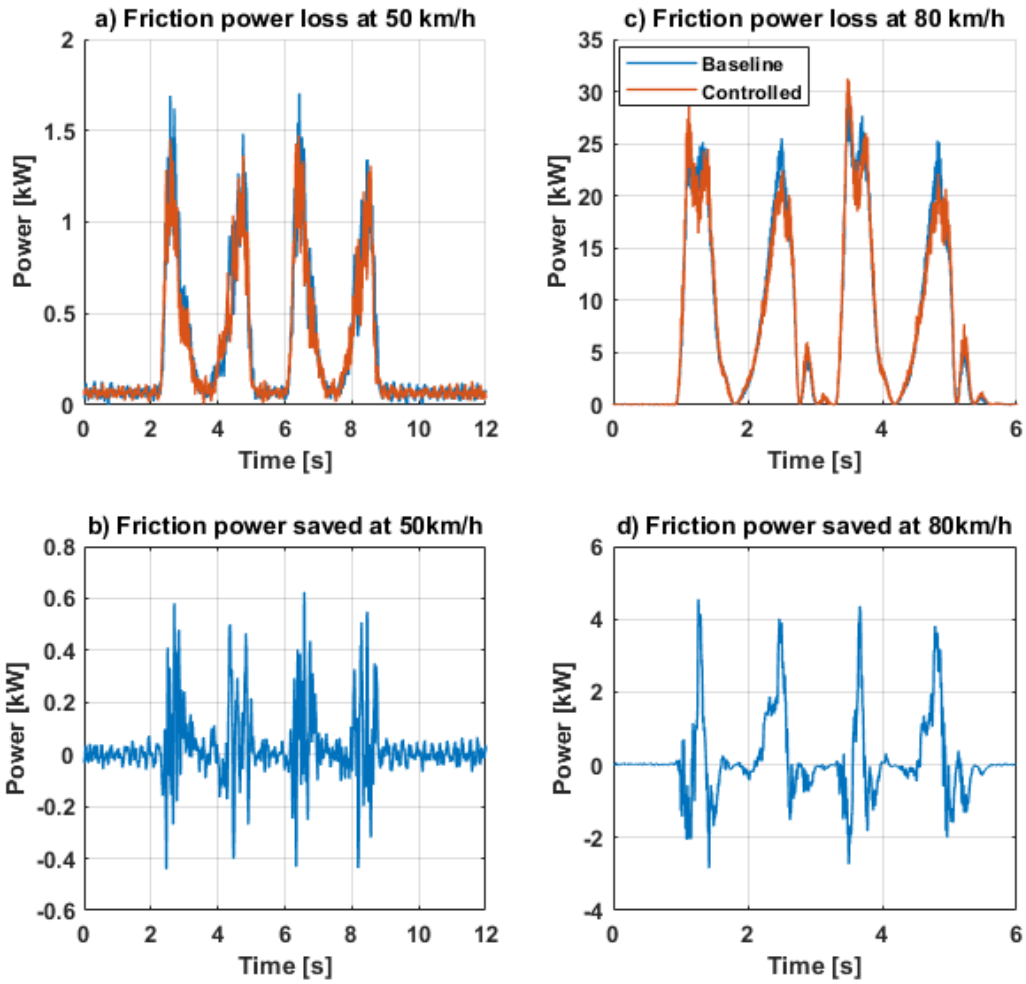

Figure 9 – Comparison of friction power loss and potential savings during severe double lane change manoeuvres at 50 km/h ((a) and (c)) and 80 km/h ((b) and (d))